

Development of the molecular design rules of ultra-permeable poly[1-(trimethylsilyl)-1-propyne] membranes

T.M. Madkour¹

ICI-Polyurethanes Research Centre, Everslaan 45, Everberg B-3078, Belgium

Received 23 August 1999; received in revised form 26 November 1999; accepted 26 January 2000

Abstract

Poly[1-(trimethylsilyl)-1-propyne] (PTMSP) is known to have the highest permeability coefficients for glassy polymers. However, unlike other glassy membranes such as polycarbonates or polysulfones, the high permeability of PTMSP decays as a function of time. A series of measurements of the gas permeability coefficients were reported in this work to highlight the effect of the physical ageing on the permeability of N₂ gas molecules through PTMSP membranes. In order to develop the molecular design rules for this high permeability, and the molecular structural parameters mostly responsible for the physical ageing, molecular dynamics techniques were used to investigate the effect of the presence of the double bond, the Si-atom, the bulky trimethylsilyl side group, the co-operative effect of the singular methyl and the trimethylsilyl side groups on the diffusion coefficients of nitrogen and argon through the polymer. It was shown that a combination of a high volume fraction, high torsion barriers around the single bonds in the main backbone and high specific electrostatic interactions due to the presence of the Si-atom are all necessary for high diffusion coefficients of gases through PTMSP membranes. This combination was also shown to provide the necessary voids for the diffusion process as well as for characterising the polymer with low cohesive energy densities and extra rigidity resulting in an exceptionally high permeability. Loss in free-volume due to the physical ageing may thus lead to lower permeability coefficients. © 2000 Elsevier Science Ltd. All rights reserved.

Keywords: PTMSP; Permeability; Diffusion

1. Introduction

Gas permeability in poly[1-(trimethylsilyl)-1-propyne] (PTMSP) is orders of magnitude larger than in other glassy polymers such as polycarbonates [1]. However, unlike other glassy polymeric membranes, gas permeability in PTMSP increases even further as the temperature is reduced. Colourless and electrically non-conductive PTMSP of molecular weights around 10⁵–10⁶ g mol⁻¹ could be obtained from solution polymerisation of 1-(trimethylsilyl)-1-propyne using niobium and tantalum catalysts [1,2]. The colourlessness and the loss of the electrical conductivity was attributed to the absence of conjugation due to the steric hindrance of the methyl and trimethylsilyl substituent groups that forces the double bonds to twist out of coplanarity. Based on solubility, permeability and other data, Srinivasan et al. [3] have concluded that fast diffusion (and not a large solubility) is responsible for the large gas permeability observed for PTMSP. The fast diffusion was reported to depend on the presence of microvoids in the

polymer and on the high connectivity among the voids [4,5]. It is thus expected that the microvoids in PTMSP form the dispersed phase, as the dense region forms the continuous phase which renders PTMSP as a loosely packed network of polymer chains with continuous channels or pores for diffusion. This is probably caused by the presence of the double bonds, which forces the polymer to possess a rigid backbone. In addition, the torsional energy barriers for rotation about a backbone single bond are rather high (~40 kcal mol⁻¹) as was calculated by Clough et al. [6], thus causing the rotation around the single bond extremely unlikely and the PTMSP chains to be viewed as inflexible coils. According to X-ray diffraction data [7] and thermal analysis measurements [8], PTMSP is an amorphous polymer with no evidence of a glass transition temperature up to 300°C. In fact, mechanical measurements [8,9] place the modulus of PTMSP between those of typical glassy and rubbery materials.

The high permeability and high selectivity of PTMSP membranes makes it ideal for industrial vapour separations. However, gas transport properties of PTMSP are somewhat unstable. Its high permeability decreases dramatically with time due to physical ageing, sorption of condensable

¹ On leave of absence from Department of Chemistry, Helwan University, Cairo, Egypt 11795.

contaminants from the environment and chemical ageing [10,11]. Jia and Baker [12] have attempted to produce mechanically stable PTMSP films by crosslinking the polymeric chains using bis(aryl azides). The films were cast from toluene solutions and had permeability and separation factors comparable or higher than those of poly(dimethylsiloxane) (PDMS) but of lower values than the uncrosslinked homopolymer. This is since crosslinking increases the local segment density and, therefore, lowers the excess free-volume fraction responsible for the high permeability. Using molecular dynamics techniques, Jo and Tang [13] have observed that the more-flexible PDMS chains have relaxed more quickly than the more-glassy PTMSP chains and thus had lower diffusion coefficients and lower selectivity between the smaller and larger penetrants. They have concluded that the difference in chain flexibility between the two polymers affects the diffusive motion of the small molecules, not by conformational relaxation but by thermal fluctuation, which seemed to be a crucial process to give the pathways for light gases to diffuse in both PTMSP and PDMS. Fried and Goyal [14] have also applied molecular dynamics techniques using the bonded constants in the DREIDING forcefield, which was parameterised for PTMSP from AM1 calculations of the dimer. The bonded constants were validated through the simulation of amorphous cell density and X-ray data (d-spacing) and used to calculate diffusion coefficients and the sorption isotherms for different gases permeating through PTMSP polymers. They obtained an excellent agreement for the diffusion and solubility coefficients for O₂, N₂ and CH₄ in PTMSP using the optimised DREIDING forcefield parameters. Trajectory analysis suggested that gas permeation in PTMSP occurs probably through large inter-chain regions formed by the rigid chains of PTMSP which could be well described by the dual-mode model for sorption (*S*) of gasses in glassy polymers, given by: [15]

$$S \equiv C = K_d a + C'_H \frac{ba}{1 + ba} \quad (1)$$

where *a* is the relative penetrant pressure, p/p^* (equal to the thermodynamic activity of an ideal gas). The concentration of penetrant in the polymer (*C*) has the units of mass of vapour sorbed per mass of polymer. The Henry's law parameter, *K_d*, is identified with penetrant sorption into the densified equilibrium matrix of the polymer, whereas the Langmuir capacity parameter, *C'_H*, characterises the sorption capacity of the non-equilibrium excess free-volume associated with the glassy state of the polymer. Finally, the Langmuir affinity, *b*, is an equilibrium constant characterising the affinity of the penetrant for a Langmuir site in the polymer.

Though there has been a considerable work done to study the high permeability of PTMSP membranes caused by fast diffusion, little was done to assess the effect of physical ageing on the permeability of light gases through PTMSP or in understanding the molecular origin of this high perme-

ability. It is the purpose of this work to develop the molecular design rules responsible for this high permeability using molecular dynamics techniques of various model systems in direct relation with the molecular structure of PTMSP. The effect of physical ageing on this high permeability will also be investigated experimentally to predict the major molecular parameters responsible for the permeability loss in PTMSP.

2. Experimental

2.1. Materials

PTMSP, kindly supplied by Gelest, Inc., PA, was used as received. Dense films of the homopolymer were prepared by casting a 2 wt% solution of the polymer in toluene onto a glass plate. The films were dried at ambient conditions for 24 h and then placed in a vacuum oven at 40°C for 48 h. The final thickness of the dried films was approximately 100 μm.

2.2. Measurement of the gas permeability coefficients

Permeability coefficients for N₂ gas molecules through PTMSP membranes were measured by the variable volume method using ASTM procedure D-1434 [16]. The permeability (*P*) was calculated using the following formula:

$$P = \frac{(\text{quantity of permeate})(\text{film thickness})}{(\text{area})(\text{time})(\text{pressure drop across film})} \\ = \frac{\text{cm}^3(\text{S.T.P.}) \text{ cm}}{\text{cm}^2 \text{ s cm Hg}} \quad (2)$$

for which quantity of permeate, film thickness, film area, permeate time and pressure drop across film need to be determined. The volume of the gas transmitted across the membrane, which represents the quantity of permeate, can be calculated after being converted to standard conditions. A micrometer was used to measure the membrane thickness to the nearest 1 μm using a minimum of eight points distributed over the entire test area. The temperature of the sample cell was controlled to a precision of ±0.1°C by means of a Neslab Exacal Ex-100 circulating bath (with ethylene glycol as the bath fluid) and a Neslab Cryocool CC-100 immersion cooler.

3. Computational methodology

For the molecular dynamics study of the various polymeric systems, a simulation model similar to that used by Depner and Schürmann [17] for aromatic polyesters was employed.

The polymer segments are subject to the bond-stretching potential, *E_b*:

$$E_b = \frac{1}{2} K_b (l - l_0)^2 \quad (3)$$

Table 1
Partial charges [14] of the various atoms comprising PTMSP dimer structure (numbers are in accordance with Fig. 1)

| Atom number | Partial charge | Atom number | Partial charge |
|-------------|----------------|--------------------------|----------------|
| Si(1) | 1.221 | C(3) | -0.031 |
| Si(5) | 1.241 | C(4) | -0.410 |
| C(19, 24) | 0.06 | C(18) | -0.380 |
| C(2) | -0.410 | C(6, 10, 14, 29, 33, 37) | -0.290 |

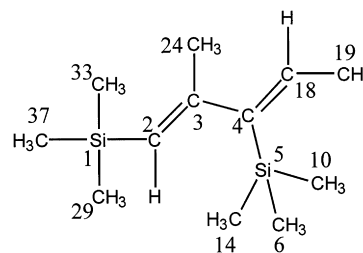


Fig. 1. Structure of the PTMSP dimer structure.

where l_0 is the equilibrium bond length and K_b the bond stretching constant. The deformation of the bond angle θ between successive pairs of bonds from its equilibrium value θ_0 is governed by the potential E_θ :

$$E_\theta = \frac{1}{2} K_\theta (\cos \theta - \cos \theta_0)^2 \quad (4)$$

with K_θ being the bond-bending constant. The torsional potential, E_ϕ , is modelled as

$$E_\phi = K_\phi [1 + \cos(n\phi - \tau)] \quad (5)$$

where K_ϕ is the torsional constant, height of the energy barrier, n is the periodicity and τ the phase angle. Out-of-plane deformations modelled as a special case of the torsion equation with $\tau = 0$ and $n = 2$ and is given by, E_x [18]:

$$E_x = K_x [1 + \cos(2\phi)] \quad (6)$$

The out-of-plane potential acts to keep the connected atom in the plane defined by the other three atoms. K_x is the out-of-plane deformation constant. Non-bonded Lennard-Jones interactions between atoms separated by more than three bonds are given by E_{nb} :

$$E_{nb} = \begin{cases} 4\epsilon^* \left[\left(\frac{r^*}{r_{ij}} \right)^{12} - \left(\frac{r^*}{r_{ij}} \right)^6 \right] + C & \text{for } r_{ij} = 1.5r^* \\ 0 & \text{for } r_{ij} > 1.5r^* \end{cases} \quad (7)$$

The Lennard-Jones parameters between different atoms A and B are assumed to satisfy the Lorentz–Berthelot mixing rules defined by

$$r_{AB}^* = (r_A^* + r_B^*)^{1/2} \quad \text{and} \quad \epsilon_{AB}^* = (\epsilon_A^* \epsilon_B^*)^{1/2} \quad (8)$$

where r^* and ϵ^* are the Lennard-Jones radius and potential.

Electrostatic interactions between atoms carrying partial charges are given by E_{ij} :

$$E_{ij} = \frac{q_i q_j}{4\pi \epsilon r_{ij}} \quad (9)$$

where q_i and q_j are the partial atomic charges on atoms i and j , respectively, r_{ij} is the distance between them and ϵ the dielectric constant. The partial charges calculated [14] using the semiempirical molecular orbital method, MNDO, are listed in Table 1. An “all-atom” forcefield was used, i.e. all the hydrogen atoms were all explicitly considered. All parameters pertaining to the simulations were optimised by Fried and Goyal [14] for the DREIDING forcefield. K_b , Eq.

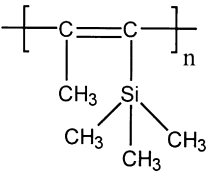
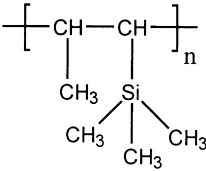
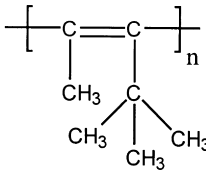
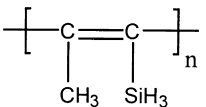
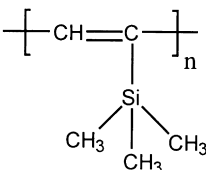
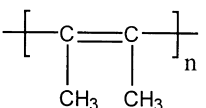
(3), of the Si–CH₃ bond, was calculated to be 361 kcal mol⁻¹ Å⁻², whereas K_θ , Eq. (4), of CH₃–C–C bond angle was taken as 218 kcal mol⁻¹ rad⁻². Results of the quantum mechanics calculations for the torsional angle CH₃–Si–C=C using the quantum mechanics method, AM1 and the simple dimer structure shown in Fig. 1 indicated a barrier of less than 5 kcal mol⁻¹ for this torsion. A single polymer chain of 50 repeat units was used in order to minimise the effect of chain ends on the results of the simulation. Initial configurations with periodic boundary conditions were generated in the simulation box as to enable the simulations to be carried out on relatively small molecular systems in such a way that the atoms experience forces as if they were in the bulk phase. In order to enhance the sampling efficiency in calculating the diffusion coefficients, 10 gaseous molecules of each type were inserted into the cells. This was done to ensure a reliable representation of the trajectories. The equilibrium molecular dynamics simulations were usually performed using microcanonical ensembles at a temperature of 298 K. Newton’s equations of motion of polymer segments were integrated [19] using the Verlet algorithm with small finite time steps ($\Delta t = 0.5 \times 10^{-15}$ s). For every structure, the simulations were run several times; usually four runs, for better averaging. The self-diffusion coefficients of the polymer were calculated from the Einstein relation [19]:

$$D_o = \frac{1}{6N} \lim_{t \rightarrow \infty} \frac{d}{dt} \sum_{i=1}^N \langle [\mathbf{r}_i(t) - \mathbf{r}_i(0)]^2 \rangle \quad (10)$$

where \mathbf{r}_i is the position vector of atom i and N is the number of all atoms in the chain. The angular brackets denote averaging over all choices of time origin and over all particles and expressed in all the figures as error bars referring to the standard errors. The diffusion coefficients of the penetrant molecules were only considered in evaluating the permeability through the different structures since it was reported [3] that the fast diffusion (and not a large solubility) is responsible for the large gas permeability observed for PTMSP.

The systems under study are the six different polymeric structures shown in Table 2, which relate to the basic molecular structure of PTMSP, structure 1. The other five structures were chosen to highlight the effect of the molecular structural parameters on the diffusion of light gases

Table 2
The various polymeric structures used as model systems for the molecular dynamics study

| Structure | Chemical formula |
|-----------|---|
| 1 |  |
| 2 |  |
| 3 |  |
| 4 |  |
| 5 |  |
| 6 |  |

through PTMSP in order to determine the most influential ones and to develop the molecular design rules for the high permeability. These parameters are: (i) the double bond in the main backbone of the polymer chain as replaced by a single bond, structure 2; (ii) the presence of an Si-atom in the side group as replaced by a C-atom, structure 3; (iii) the three methyl groups attached to the Si-atom as replaced by H-atoms, structure 4; (iv) the singular methyl group on the side chain as replaced by a H-atom, structure 5; and (v) the bulky trimethylsilyl

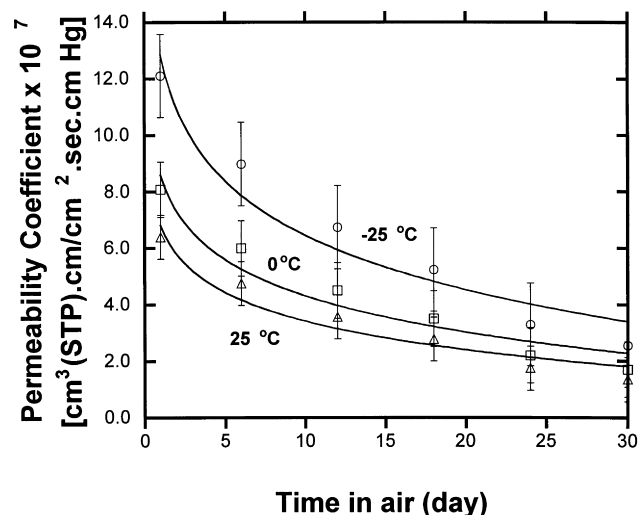


Fig. 2. Effect of ageing time on the permeability coefficients of N_2 in PTMSP membranes at different temperatures.

side group as replaced by a methyl group, structure 6, representing polyacetylene.

4. Results and discussion

4.1. Experimental results

Fig. 2 indicates the effect of ageing time on the permeability coefficients of N_2 in PTMSP membranes at different temperatures, namely, -25 , 0 and 25°C . It is obvious from the figure that the effect of ageing on the permeability of N_2 through PTMSP membranes levels off by time. This indicates a possible physical chain packing which increases the local segment density and lowers the excess free-volume responsible for high permeability. Temperature had a similar effect; increasing the temperature has resulted into decreasing the permeability coefficient, opposite to the permeability behaviour in glassy polymers. It is interesting to observe that this decrease was consistent over the full range of time used to test these samples.

4.2. Computational results

As was shown above, the physical ageing tested for a series of PTMSP samples has indicated a possible physical effect on the chain packing. In other words, there must be one or more molecular structural parameters that might allow the polymer to increase its local segment density with time and the subsequent effect on the excess free-volume. Using molecular dynamics techniques, it might thus be possible to determine which parameters are the most influential on the observed high permeability of PTMSP and on the continuing ageing process as a function of the fractional free-volume.

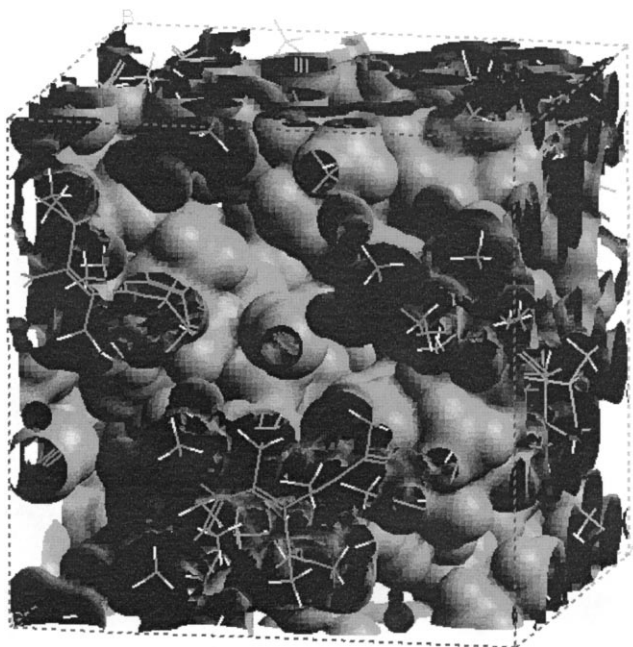


Fig. 3. Schematic presentation of the free-volume isosurface.

4.2.1. Free-volume

In order to study the free-volume size and distribution in bulk simulated molecular models, the hard probe method was used [20]. In this method, the periodic box was divided into $100 \times 100 \times 100$ cubic subcells. All of the atoms were assumed to be hard spheres with radii equal to 88% of the full van der Waals radii. Each subcell was then scanned to screen out the occupied subcells. The subcell was labelled as “occupied” whenever more than half of the subcell size lay within any hard sphere. After checking occupancy, a probe, which is also assumed to be a hard sphere, was introduced at the centre of an unoccupied subcell. Each unoccupied subcell was determined to be “inaccessible” if more than half of any occupied subcell size lay within the spherical probe. The inaccessible subcells were classified as occupied subcells as well. According to Mattice et al. [21] connectivity is formed when two unoccupied subcells having connectivity were assigned to the same void. The total unoccupied volume of the cell divided by the total volume of the cell is thus defined as the fractional free-volume of that cell.

Fig. 3 shows a schematic representation of an isosurface encompassing the free-volume in a 3D-periodic cell containing a single PTMSP chain. Fig. 4 indicates a comparison between the calculated properties of the six different structures shown in Table 2. The first column of every data set in Fig. 4 represents the fractional free-volume calculated according to the above described methodology. It is apparent that varying the molecular structural parameters had a slight effect on the free-volume. The most apparent effect was due to the replacement of the double bond in the main backbone by a single bond, which is the result of the chain becoming more flexible, which allows the chains to relax more efficiently resulting in an increase in the local segment

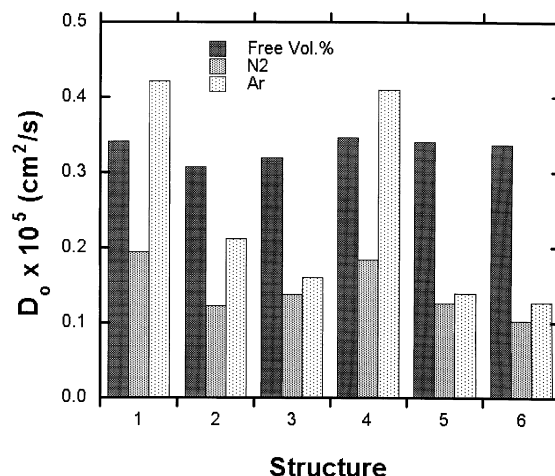


Fig. 4. The diffusion coefficients of N₂ and Ar through PTMSP in comparison to the fractional free-volume values.

density. Replacing the silicon atom by a carbon atom also resulted in lowering the free-volume, possibly due to the smaller van der Waals parameters of the latter (Eqs. (7) and (8)). Other changes did not result into a major decrease in the free-volume of the system which indicates that the system retains its rigidity due to the presence of the double bond in the backbone of the chain and the presence of the partially charged Si-atom on the side chain.

In order to relate the findings of the free-volume investigation to the difference in the diffusion coefficients of the various structures, molecular dynamics techniques were used to evaluate the diffusion coefficients of permeating N₂ molecules through the different polymeric structures. However, specific electrostatic interactions between the nitrogen atoms and the polymer might add to the complexity of relating the difference in the diffusion coefficients to the free-volume available to the system. Therefore, noble gases will also be used in this study since they have little interaction with the polymer and any conclusions about the diffusion of the noble gases into the polymer should only be on the basis of the free-volume effect. The noble gas that will resemble N₂ the most, should have a Connolly surface of a close value to that of N₂.

4.2.2. Connolly surface

A Connolly surface [22] is the van der Waals surface of the model that is accessible to a solvent molecule having a non-zero radius. The surface is generated by rolling a spherical probe of a specified radius over the van der Waals surface of the models. Table 3 lists the Connolly surface of N₂ and that of the different noble gases. It is apparent from the table that argon has the closest value to that of N₂ for the Connolly surface. Fig. 5 is a schematic representation of the Connolly surfaces of Ar and N₂.

Determination of the diffusion coefficients of Ar, N₂ and the self-diffusion coefficients of the various polymeric structures was achieved using Eq. (10). Figs. 6–11 represent,

Table 3
Connolly surfaces of N₂ and various noble gases

| Gas | Connolly surface (Å ²) |
|----------------|------------------------------------|
| N ₂ | 40.002 |
| He | 24.630 |
| Ne | 29.802 |
| Ar | 44.415 |
| Kr | 51.276 |
| Xe | 58.630 |

respectively, the mean-square displacements of the polymer atoms and the penetrant molecules for the six different structures shown in Table 2. Values of the diffusion coefficients calculated from Figs. 6–11 for the six different structures are shown in Fig. 4. Few observations could be made regarding the effect of the various molecular structural parameters on the diffusion coefficients.

(i) *PTMSP molecular structure*: Fig. 6 and the first data set in Fig. 4 indicate the higher diffusion coefficient for Ar through PTMSP when compared to that of N₂. This is probably due to the lower amount of electrostatic interaction between the penetrant molecules and the polymer

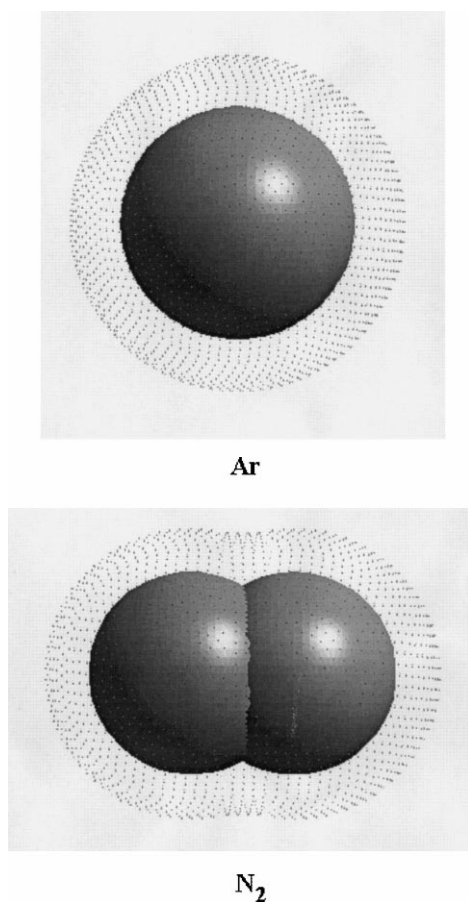


Fig. 5. Schematic presentation of Connolly surfaces of N₂ and Ar gas molecules.

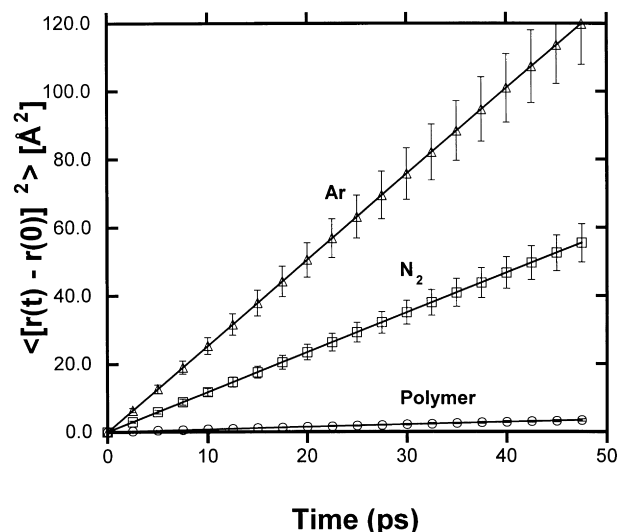


Fig. 6. Mean-square displacements of the polymer segments and penetrant molecules as a function of time of PTMSP.

chains. Furthermore, Fig. 6 indicates a very low self-diffusion coefficient of the polymer as a result of the rigidity of the polymer.

(ii) *Effect of the double bond in the main backbone of the polymer chain*: Fig. 7 and the second data set in Fig. 4 clearly show the drop in the diffusion coefficient of Ar through the polymer. This is also accompanied to a lesser extent by a similar drop for the diffusion coefficient of N₂. The absence of the double bond has removed some of the rigidity of the polymeric chain, lowered the free-volume fraction and subsequently the diffusion coefficients.

(iii) *Effect of the Si-atom on the side group*: Replacement of the Si-atom by the smaller and less-electrostatic C-atom

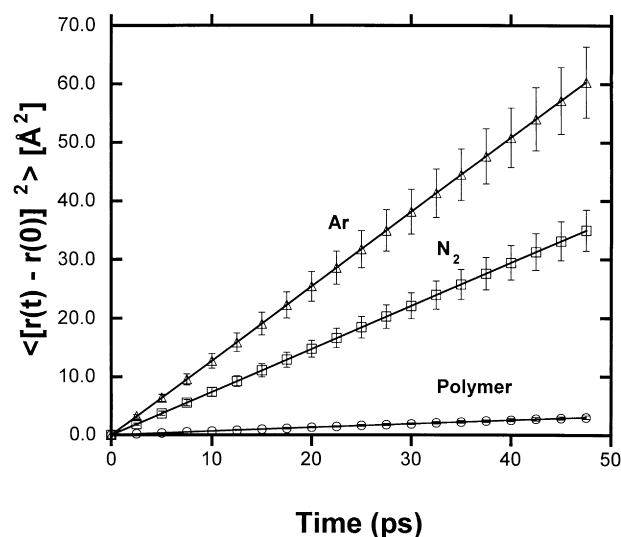


Fig. 7. The effect of replacement of the double bonds by single ones in the main backbone on the mean-square displacements of the polymer segments and penetrant molecules as a function of time.

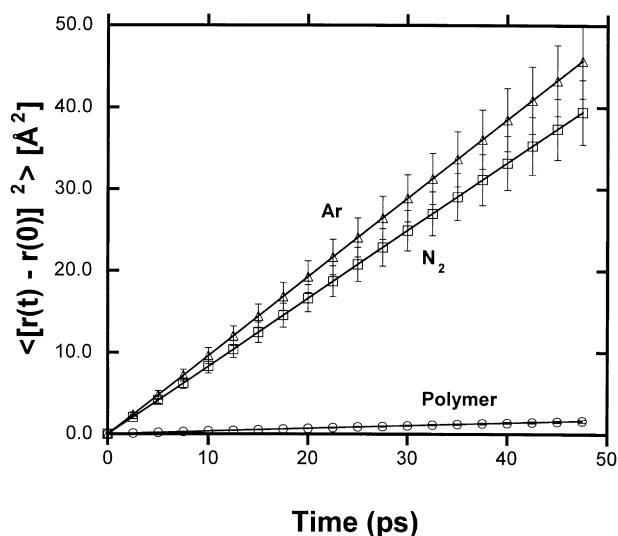


Fig. 8. The effect of replacement of the Si-atoms by C-atoms in the side chain on the mean-square displacements of the polymer segments and penetrant molecules as a function of time.

in the trimethylsilyl side group has resulted, as shown in Fig. 8 and the third data set in Fig. 4, in decreasing the diffusion coefficient of Ar and N_2 with respect to those of PTMSP. This is also in conjunction with a slight increase in the polymer self-diffusion coefficient and a slight decrease in the fractional free-volume. More importantly, the diffusion coefficients of both N_2 and Ar are quite similar for this structure, probably since the polymer has no obvious electrostatic interactions due to the absence of the Si-atom. Nevertheless, Ar, with little electrostatic interaction, was more affected by the absence of the Si-atom than N_2 was, which indicates an indirect effect of the interaction of the local polymeric segments with each other on the motion of the uncharged Ar molecules.

(iv) *Effect of the three methyl groups attached to the Si-atom:* Fig. 9 and the fourth data set in Fig. 4 indicate, surprisingly, that the replacement of the bulky trimethylsilyl side group by the smaller SiH_3 group did not result into a noticeable change on the free-volume of the polymer or on the diffusion coefficients of N_2 and Ar. This probably indicates that the electrostatic charges of the Si-atom in this group have a more predominant effect on the permeability of the light gases through the polymer when compared to the bulkiness of the side group.

(v) *Effect of the singular methyl side group:* Fig. 10 and the fifth data set in Fig. 4 indicate the importance of the presence of the methyl side group in maintaining the high permeability of the light gases through PTMSP. This is possibly because of its effect in increasing the rigidity of the polymeric chain and promoting high torsional barrier for rotation around the single bond in the main backbone of the chain.

(vi) *Polyacetylene molecular structure:* Finally, Fig. 11

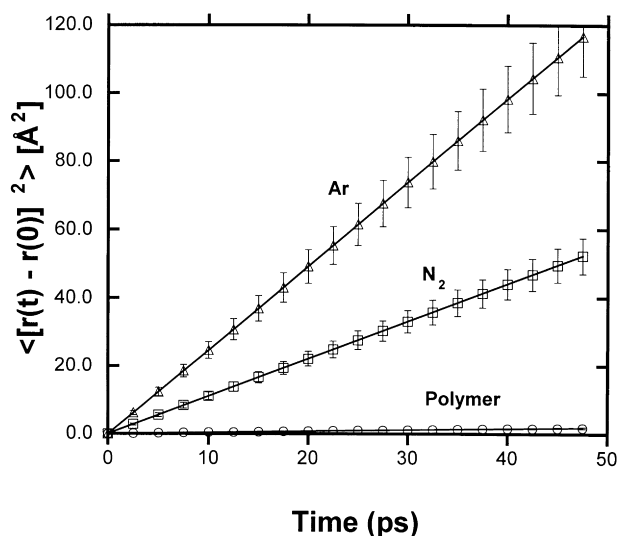


Fig. 9. The effect of replacement of the three methyl groups of the side group on the mean-square displacements of the polymer segments and penetrant molecules as a function of time.

and the last data set in Fig. 4 indicate that polyacetylene has a much lower diffusivity for light gases when compared to PTMSP, most probably because of the absence of the silicon atom.

Considering the above observations, along with the earlier ones made regarding the effect of the physical ageing on the permeability of N_2 through PTMSP, it could be deduced that physical ageing must affect the polymer through a better packing of the chains, thus lowering the fractional free-volume through the increase in the local segment density. The presence of the Si-atom, the methyl side group and the double bond in the main backbone

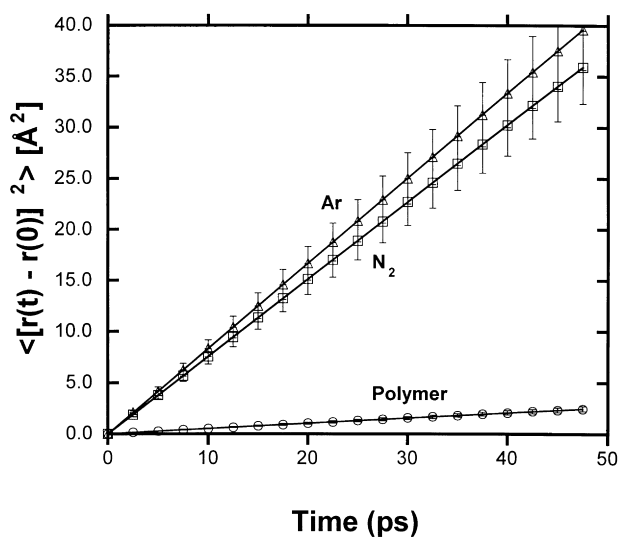


Fig. 10. The effect of replacement of the singular methyl group on the side chain on the mean-square displacements of the polymer segments and penetrant molecules as a function of time.

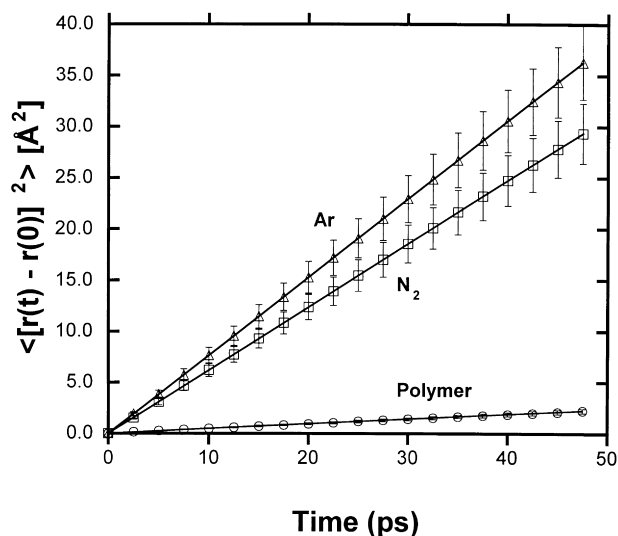


Fig. 11. Mean-square displacements of the polymer segments and penetrant molecules as a function of time of polyacetylene.

of the polymer were all essential in promoting the high permeability in PTMSP since it is not only the fractional free-volume that is solely responsible for the high diffusion coefficients. In order to emphasise on this point, we consider the breakdown of the total energies of the systems during the molecular dynamics runs. Tables 4 and 5 list the major energy terms constituting the total energy expression of the various polymeric structures. It is obvious from the tables that a combination of a high volume fraction, high torsion barriers around the single bonds in the main backbone and high specific electrostatic interactions are all

necessary for high diffusion coefficients of gases through PTMSP membranes. These combinations were shown to provide the necessary voids for the diffusion process as well as for characterising the polymer with low cohesive energy densities and extra rigidity resulting in an exceptionally high permeability.

5. Conclusions

Permeability of N_2 gas molecules through PTMSP membranes showed exceptionally high permeability coefficients that decay as a function of time. Molecular dynamics techniques were thus used to evaluate the molecular structural parameters most responsible for the high permeability and for the physical ageing of the material caused by the loss in the free-volume. It was shown that a combination of a high volume fraction, high torsion barriers around the single bonds in the main backbone and high specific electrostatic interactions are all necessary for high diffusion coefficients of gases through PTMSP membranes. It was also shown that Ar had a higher diffusion coefficient through PTMSP than that of N_2 molecules, which is probably due to the electrostatic interactions present between the Si-atom of PTMSP and the N_2 gas molecules. This was further shown by replacing the Si-atom on the trimethylsilyl side group, which resulted into a massive decrease in the diffusion coefficients of both gases. Replacing the three methyl groups on the same side group by H-atoms, thus decreasing its size extensively, did not result into a similar effect on the diffusion coefficients or the fractional free-volume. The free-volume is certainly necessary for high diffusion coefficients but it

Table 4

Major energy terms constituting the total energy expression of the various polymeric structures in case of the diffusion of N_2

| Structure | Bond | Angle | Torsion | van der Waals | Electrostatic | Total | N_2 diff. coeff. ^a |
|-----------|---------|---------|----------|---------------|---------------|----------|---------------------------------|
| 1 | 356.828 | 778.089 | 1105.14 | 5.09528 | -1825.89 | 345.231 | 0.1947 |
| 2 | 384.225 | 795.238 | -329.844 | -145.108 | -1392.45 | -856.188 | 0.1227 |
| 3 | 518.713 | 818.186 | 1038.65 | 385.718 | -383.320 | 2267.53 | 0.1383 |
| 4 | 208.366 | 280.695 | 884.472 | 154.195 | -598.543 | 942.277 | 0.1835 |
| 5 | 222.915 | 691.663 | 491.063 | -127.790 | -886.367 | 337.522 | 0.1260 |
| 6 | 214.094 | 379.693 | 763.206 | 176.429 | 12.2594 | 1488.24 | 0.1030 |

^a Included for highlighting the dependence of the diffusion of N_2 on the various energy terms.

Table 5

Major energy terms constituting the total energy expression of the various polymeric structures in case of the diffusion of Ar

| Structure | Bond | Angle | Torsion | van der Waals | Electrostatic | Total | Ar diff. coeff. ^a |
|-----------|---------|---------|----------|---------------|---------------|----------|------------------------------|
| 1 | 349.097 | 761.823 | 1102.12 | -4.63848 | -1826.54 | 329.134 | 0.4209 |
| 2 | 361.712 | 815.561 | -340.255 | -142.507 | -1396.62 | -870.708 | 0.2117 |
| 3 | 515.755 | 777.565 | 1128.13 | 317.076 | -383.496 | 2267.70 | 0.1603 |
| 4 | 210.935 | 285.286 | 928.344 | 105.999 | -596.397 | 941.835 | 0.4098 |
| 5 | 259.079 | 748.835 | 449.092 | -128.655 | -887.628 | 370.720 | 0.1389 |
| 6 | 235.383 | 341.859 | 818.713 | 171.118 | 11.1783 | 1522.96 | 0.1273 |

^a Included for highlighting the dependence of the diffusion of Ar on the various energy terms.

was shown that it must be accompanied by specific electrostatic interactions, which gives rise to a low cohesive energy for the polymer, and high torsion barriers around the single bond resulting into highly rigid polymeric conformations.

Acknowledgements

The author would like to thank Gelest, Inc., PA, for providing the necessary PTMSP samples.

References

- [1] Madkour TM. In: Mark JE, editor. Polymer data handbook, New York: Oxford University Press, 1999. p. 863.
- [2] Masuda T, Higashimura T. *Adv Polym Sci* 1985;18:841.
- [3] Srinivasan R, Auvil SR, Burban PM. *J Membr Sci* 1994;86:67.
- [4] Maxwell JC. *A treatise on electricity and magnetism*. 3rd ed.. London: Clarendon Press, 1904.
- [5] Cussler EL. *Diffusion–mass transfer in fluid systems*. London: Cambridge University Press, 1984.
- [6] Clough SB, Sun XF, Tripathy SK, Baker GL. *Macromolecules* 1991;24:4264.
- [7] Takada K, Matsura H, Masuda T, Higashimura T. *J Appl Polym Sci* 1985;30:1605.
- [8] Masuda T, Tang BZ, Tanaka A, Higashimura T. *Macromolecules* 1986;19:1459.
- [9] Langsam M, Robeson LM. *Polym Engng Sci* 1989;29:44.
- [10] Odani H, Masuda T. In: Toshima N, editor. *Polymers for gas separation*, VCH: New York, 1992. p. 107.
- [11] Nagai K, Nakagawa T. *J Appl Polym Sci* 1994;54:1651.
- [12] Jia J, Baker GJ. *J Polym Sci B: Polym Phys* 1998;36:959.
- [13] Jo W, Yang J. *Polym Prepr* 1997;38:173.
- [14] Fried J, Goyal DJ. *J Polym Sci B: Polym Phys* 1998;36:519.
- [15] Morisato A, Freeman B, Pinnau I, Casillas CJ. *J Polym Sci B: Polym Phys* 1996;34:1925.
- [16] ASTM, D1434-82, American Society for testing and Materials, 1990 (reapproved 1988).
- [17] Depner M, Schürmann BL. *Polymer* 1992;33:398.
- [18] Madkour TM. *Polym J* 1997;29:670.
- [19] Allen MP, Tildesley DJ. *Computer simulation of liquids*. Oxford: Clarendon Press, 1987.
- [20] Rigby D, Roe RJ. *Macromolecules* 1990;23:5312.
- [21] Kim WK, Mattice W. *Comput Theor Polym Sci* 1998;8:353.
- [22] Connolly ML. *J Appl Crystallogr* 1983;16:548.